

Structural Examination of Easel Paintings with Optical Coherence Tomography

PIOTR TARGOWSKI,^{*†} MAGDALENA IWANICKA,[†]
LUDMIŁA TYMIŃSKA-WIDMER,[‡] MARCIN SYLWESTRZAK,[†] AND
EWA A. KWIATKOWSKA[†]

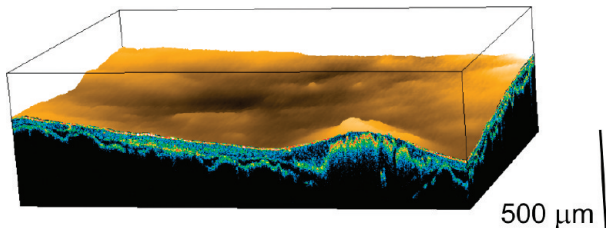
^{*}Institute of Physics, Nicolaus Copernicus University, ul. Grudziadzka 5,
87-100 Toruń, Poland, [‡]Institute for the Study, Restoration and Conservation of
Cultural Heritage, Nicolaus Copernicus University, ul. Gagarina 7,
87-100 Toruń, Poland

RECEIVED ON JULY 6, 2009

© This paper contains enhanced objects available on the Internet at <http://pubs.acs.org/acr>.

CONSPETCUS

Identification of the order, thickness, composition, and possibly the origin of the paint layers forming the structure of a painting, that is, its stratigraphy, is important in confirming its attribution and history as well as planning conservation treatments. The most common method of examination is analysis of a sample collected from the art object, both visually with a microscope and instrumentally through a variety of sophisticated, modern analytical tools. Because of its invasiveness, however, sampling is less than ideally compatible with conservation ethics; it is severely restricted with respect to the amount of material extirpated from the artwork. Sampling is also rather limited in that it provides only very local information. There is, therefore, a great need for a noninvasive method with sufficient in-depth resolution for resolving the stratigraphy of works of art.



Optical coherence tomography (OCT) is a noninvasive, noncontact method of optical sectioning of partially transparent objects, with micrometer-level axial resolution. The method utilizes near-infrared light of low intensity (a few milliwatts) to obtain cross-sectional images of various objects; it has been mostly used in medical diagnostics. Through the serial collection of many such images, volume information may be extracted. The application of OCT to the examination of art objects has been in development since 2003.

In this Account, we present a short introduction to the technique, briefly discuss the apparatus we use, and provide a paradigm for reading OCT tomograms. Unlike the majority of papers published previously, this Account focuses on one, very specific, use of OCT. We then consider two examples of successful, practical application of the technique. At the request of a conservation studio, the characteristics of inscriptions on two oil paintings, originating from the 18th and 19th centuries, were analyzed. In the first case, it was possible to resolve some questions concerning the history of the work. From an analysis of the positions of the paint layers involved in three inscriptions in relation to other strata of the painting, the order of events in its history was resolved. It was evident that the original text had been overpainted and that the other inscriptions were added later, thus providing convincing evidence as to the painting's true date of creation. In the second example, a painting was analyzed with the aim of confirming the possibility of forgery of the artist's signature, and evidence strongly supporting this supposition is presented.

These two specific examples of successful use of the technique on paintings further demonstrate how OCT may be readily adaptable to other similar tasks, such as in the fields of forensic or materials science. In a synergistic approach, in which information is obtained with a variety of noninvasive techniques, OCT is demonstrably effective and offers great potential for further development.

Introduction

Easel paintings, especially when prepared according to traditional techniques, are multilayered structures. A support, usually stretched canvas or a wooden panel, is covered with glue size, and then primed in order to smooth its surface and to ensure proper adhesion of the consecutive layers. The composition may be outlined in an underdrawing executed by one of various techniques, and then the opaque paint layers are applied. To obtain a desirable visual effect, an additional cover of one or more layers of semitransparent glazes and finally a transparent varnish may be added. Apart from the obvious protective function of the varnish, it has a very important effect on the final appearance of the artwork.^{1,2} Additionally in many cases, this primary structure may be modified by alterations introduced by the artists themselves or commissioned by later owners. Among these, traces of previous renovation treatments, for example, overpaintings, are particularly important to detect. Another separate group of interventions in the structure of the artwork are various kinds of forgeries, sometimes committed many years or even one or more centuries ago and having their own history.

For conservation or inventory purposes, it is very important to reveal the stratigraphy, that is, the order, thickness, composition, and possibly the origin, of the layers building up the painting's structure. This knowledge is important in confirming the attribution and history of the artwork and is also essential for the planning of future conservation treatments. For these reasons, the attention of art historians and conservators has long been focused on methods of obtaining such information. The most common approach has been, and still largely is, to collect a small sample, embed it in resin, and then analyze its cross section under the microscope. At present, in addition to or replacing classical microchemical analysis,³ a wide range of microspectroscopic methods, for example, micro-Raman (μ Raman), micro-infrared Fourier transform (μ FTIR), micro-X-ray fluorescence (μ XRF), scanning electron microscopic energy-dispersive X-ray (SEM-EDX), and particle-induced X-ray emission (PIXE) spectroscopies, is used to better understand artwork composition throughout examination of the sample.⁴

However, despite the fact that the results obtained in this way have been and to a large extent still are usually considered the most unequivocal, there are two disadvantages to this approach. First, sampling is rightly regarded as invasive, and so its application is strictly limited by conservation ethics. Usually it is allowed to be performed only within an area of former damage, where collecting material would have a

negligible impact on the final condition of the artwork. Therefore, information collected this way must be considered rather random and not necessarily representative of the object as a whole. In addition, the results obtained from sampling in the area of destruction must of necessity be interpreted with extreme care, since the structure of the object in this very place could have already been more or less heavily perturbed by the damage. The second disadvantage of sampling methodologies lies in their local character: the information gained is always specific to the site of sampling, since the structure of the painting, especially the thickness of particular layers, may vary rapidly⁵ across even fairly small regions.

All of these limitations have long been known, and in response, alternative noninvasive investigations have gained significant attention. Paintings are X-rayed to detect alterations and traces of former compositions covered by later superimposed additions. The inspection of paintings by means of UV-excited fluorescence has also become very popular: not only may old paint and varnish layers (fluorescent) be distinguished from new ones (nonfluorescent),⁶ but the chemical composition of the varnish may be revealed due to the characteristic fluorescence exhibited by some of its ingredients.⁷ Visual inspection of UV-excited fluorescence may also indicate the presence of certain pigments in the paint layer.¹ Another technique used for pigment identification is reflectance spectroscopy in visible light.⁸ The significant transparency of many pigments to infrared light permits utilization of IR radiation in the wavelength range 0.7 to 7 μm ^{9,10} to reveal underdrawings.

The methods described above allow general diagnoses of paintings for the purpose of resolving causes of their deterioration and to detect damaged regions as well as areas of former conservation treatments. Information on the location of underdrawings, on regions of previous restorations, on the thickness of paint layers, and on the presence of delaminations can also be obtained through various thermographic inspection techniques, including pulsed phase thermography (PPT).¹⁰ The identification of delaminations may also be achieved through air-coupled ultrasound echo detection.¹¹ Holographic interferometry techniques provide information on bulk structural faults and mechanical discontinuities in a piece of artwork.¹² All these noninvasive methods, as well as modern structurally resolving ones like XRF (see above) or CT (computed tomography) either are only sensitive to surface properties or do not have sufficient spatial resolution to be useful for structures with an overall thickness of only a fraction of a millimeter: the resulting information comprises an overlap of that from all different depths.

This Account is devoted to a novel technique, optical coherence tomography (OCT), for high-resolution structural imaging, operational in conservation science since 2003.¹³ OCT uses low-power light in the spectral range of 700 to 1500 nm to probe structure noninvasively from a distance of a few centimeters, in order to provide detailed micrometer-resolved information on its cross section, and thus stratigraphy, in a purely optical, noncontact, noninvasive, and nondestructive way.

The major drawback to practical application of OCT in the examination of artwork arises from the limited transparency of the strata examined to the light used. However, layers like varnishes and glazes, usually semitransparent and thereby decisive for aesthetic impression, may readily be successfully tested in this way. In addition, the very high sensitivity of modern OCT modalities enables the collection of signals from deeper structures.

Until now, OCT has been employed in the investigation and conservation of artwork to examine varnish and glaze layers of easel paintings,^{14–18} analyze underdrawings,¹⁵ examine historic jades,¹⁹ ceramics, and glass objects,^{20,21} inspect atmospheric corrosion of stained glass,²² and precisely image punchwork.²³ Another group of applications is related to monitoring various dynamic processes such as the drying of a varnish layer,^{24,25} laser ablation of varnish,^{26–28} and the tracing of environmentally induced deformations of paintings on canvas.²⁹

In this Account, the application of OCT to investigation of the structure of easel paintings is revisited and extended to more practical aspects. Using examples of oil paintings from a conservation studio, it will be shown how information obtained with OCT may be used to verify their history and authenticity.

Methodology

The OCT technique originates from diagnostic medicine³⁰ and at present is used mostly in ophthalmology for examination of the human retina, though OCT tomographs are also commercially available for examination of the anterior segment of the eye and of skin and other tissues. These instruments, as well as those designed for material science, may be directly used to examine works of art.

In every OCT instrument, infrared radiation penetrates the object and is partially reflected at interfaces of layers of different refractive indices, or sometimes scattered from sites of inhomogeneity in its structure. Returning light is collected, and the time of propagation from the given depth of the structure is determined, thus providing a measurement of the opti-

cal path to this structure. However, at the micrometer path resolution desired, this propagation time cannot be measured directly and is accomplished instead through a measurement of interference between the object and reference beams in an interferometer. Many specific configurations of OCT instrumentation are described in detail elsewhere,³⁰ so only a brief summary of the principle and description of the instrument used by the authors will be given here.

To explain the general idea of the OCT device, consider the interferometer (usually of the Michelson type) with the object to be investigated in one arm and a mirror in the second (reference) arm. An original beam from the broadband light source is split into two, often propagated in optic fibers, as depicted in Figure 1. The object is penetrated by a narrow beam of light from one of them, some of which is reflected or scattered back from various elements (1, 2, ..., n) of the structure and collected in the interferometer. The second beam is simultaneously back-reflected from a reference mirror. The beam splitter recombines these beams to allow interference. If the difference of round trip propagation times in the two arms of the interferometer is τ_n for a given structural element n, the interference signal may be described by the general formula

$$I(\omega) = I_r(\omega) + \sum_n I_n(\omega) + 2 \sum_n [\sqrt{I_r(\omega)I_n(\omega)} \cos(\omega\tau_n)] \\ = S(\omega) \left\{ R_r + \sum_n R_n + 2 \sum_n [\sqrt{R_r R_n} \cos(\omega\tau_n)] \right\} \quad (1)$$

where the index r refers to the signal from the reference arm. In the first line expression, the common assumption that the (intensity) reflection coefficients R do not depend on the optical frequency ω is invoked. $S(\omega)$ denotes the spectrum of the light source.

It can be seen in eq 1 that τ_n appears as its product with the optical frequency ω . As a result, two approaches to extracting structural information (R_n and τ_n) from the interferometric signal are possible. In the first-developed method, time-domain OCT (TdOCT), the interference signal is collected by means of a photodiode and thus integrated over its spectrum. In this case, the cosine term averages to zero everywhere except at $\tau \approx 0$. More precisely, the full width at half-maximum (FWHM) of the interference signal as a function of τ defines the axial resolution of the OCT instrument. For a Gaussian-shaped light source of central wavelength λ_{center} and a spectral bandwidth $\Delta\lambda_{\text{FWHM}}$, this width, $\Delta\tau_{\text{FWHM}}$, and therefore the axial resolution, Δx , are given by the formulas

$$\Delta\tau_{FWHM} = \frac{8 \ln 2}{\Delta\omega_{FWHM}} \quad \text{and} \quad \Delta x = \frac{1}{n_R} \frac{2 \ln 2}{\pi} \frac{\lambda_{center}^2}{\Delta\lambda_{FWHM}} \quad (2)$$

where both the forward and backward directions of light propagation in the object and the refractive index, n_R , of the investigated region are taken into account in calculating Δx .

As can be seen from eq 2, the in-depth resolution increases with increasing bandwidth of the light source. Thus, to achieve the required axial resolution for these studies, broadband light sources with $\Delta\lambda_{FWHM}$ between 30 and 200 nm are utilized. Since Δx quickly increases (i.e., deteriorates) for deeper infrared radiation in the spectral range 800–1050 nm is usually employed.

In time-domain OCT, the reference mirror is moved gradually, and the interference signal is simultaneously registered to complete the in-depth scan. When the optical paths match to within Δx , an interference signal is detected. Knowing the position of the mirror, a profile of the internal structure of the object along the probing beam can be recovered. To recover complete cross sections, the probing beam is scanned over the object. By analogy with the usage in ultrasonography, such a cross-sectional image is called a B-scan, whereas the profile along a single vertical line is called an A-scan. Different images are obtained using the full-field modality of the OCT technique (FF-OCT),¹⁵ which produces cross sections in planes perpendicular to the direction of probing light (C-scans). Among the various FF-OCT systems available, microscopic devices (utilizing Linnik³¹ or Mirau¹⁷ configurations) have outstanding in-plane resolution, at the price, however, of a field of view limited to a fraction of a millimeter. Moreover, these systems very often utilize light from the visible range, which, according to eq 2, also provides better in-depth resolution.¹⁷ FF-OCT additionally holds promise for spectroscopic imaging.³²

Fourier-domain OCT was developed later³³ and differs from TdOCT in the way the structural information is extracted from the interferometric signal given by eq 1. In this case, the spectral signal is registered by means of a spectrograph (spectral OCT), or a very fast-tuned laser is used as a source with a single photodiode detector (swept source OCT). In both modalities, the spectrum of the interference signal is analyzed by means of Fourier transformation, and the components obtained have frequencies proportional to delay differences τ_n and amplitudes proportional to reflectivities R_n .

The advantages of Fourier domain methods lie in the absence of movable parts in the reference arm, which increases the acquisition speed 100-fold, and in significantly higher sensitivity due to the multiplex advantage.³⁴

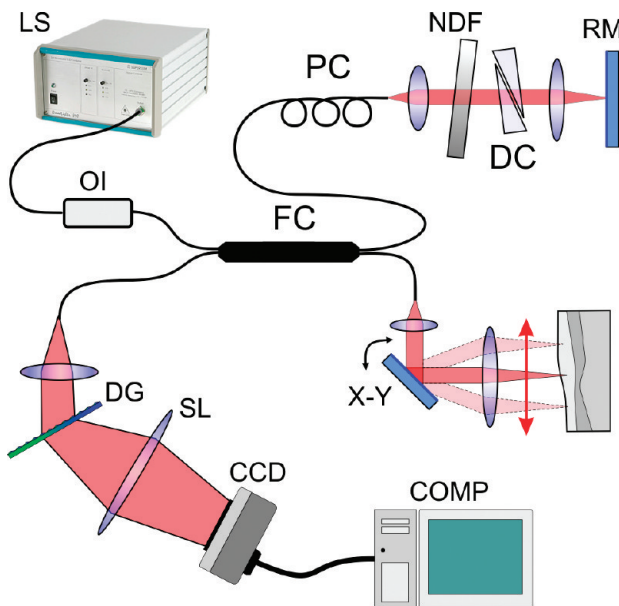


FIGURE 1. OCT tomograph used in this study: LS, light source; OI, optical isolator; FC, fiber coupler; PC, polarization controller; NDF, neutral density filter; DC, dispersion compensator; RM, reference-arm mirror; X-Y, transversal scanner; DG, diffraction grating; SL, spectrograph lens, CCD, linear CCD camera.

Another important consequence of eq 1 arises from the fact that in the interference term, $(I_r I_n)^{1/2}$, a weak useful signal I_n is multiplied by a strong reference signal I_r . This leads, due to heterodyne gain, to the very high, shot-noise limited sensitivity of the method.

In the case studies reported in this Account, a prototype laboratory-constructed high-resolution spectral OCT imaging system (tomograph) was employed (Figure 1). Its axial resolution is measured at 4 μm in air. It comprises a broadband infrared light source (LS, $\lambda_{center} = 845 \text{ nm}$, $\Delta\lambda_{FWHM} = 107 \text{ nm}$) made up of two superluminescent diodes coupled together. The light output, of high spatial coherence (ensuring sensitivity), is launched into a single-mode optical fiber and passed through an optical isolator (OI), which protects the source from back-reflected light. This tomograph employs a fiber-optic Michelson interferometer, comprising a 50:50 fiber-optic coupler (FC) dividing the light into reference and object arms. The reference arm includes a polarization controller (PC), which provides optimal polarization conditions for interference, a neutral density filter (NDF) for adjusting the light power to achieve shot-noise-limited detection, a block of glass (DC) acting as a dispersion compensator, and the stationary reference mirror (RM). The object arm comprises a lens forming a narrow probing beam and a transversal scanner (X-Y) responsible for scanning the beam across the sample. The light beams, back-reflected from the reference mirror and reflected and or

backscattered from structural elements of the object, return to the coupler and interfere.

To extract structural information from the interference signal, the tomograph is equipped with a custom-designed spectrograph employing a fast CCD camera as detector. The spectrograph comprises a volume-phase holographic grating (DG) with 1200 grooves/mm and an achromatic lens (SL), which focuses the spectrum onto a 12-bit single-line CCD camera (2048 pixels, 12-bit A/D conversion). Following Fourier transformation, the interference signal yields an A-scan, that is, one line of the cross-sectional image. Moving the beam across the sample in the X or the Y direction with the transversal scanner (X-Y) enables collection of a B-scan, that is, a 2-D cross-sectional image, while the addition of scanning in the perpendicular direction (Y or X, respectively) yields complete 3-D information on the spatial structure within seconds.

Cross-sectional images obtained by OCT are usually presented in a false-color scale: black areas correspond to non-scattering media, such as air or clear, transparent varnish. Cold colors (blue and green) indicate low-scattering or reflecting areas, whereas warm colors (yellow and red) designate high-scattering or -reflecting regions. More details on mapping the scattered or reflected intensities with false colors may be found elsewhere.³⁵

In all tomograms shown here, the incident light path is from the top, through air. Thus, the first strong line corresponds to the air–painting (i.e., most usually the air–varnish) interface, while other layers accessible by the light utilized appear below this. The lowest layer depicted is always the first nontransparent one in the structure.

It must be emphasized that all distances within an object are presented in the OCT tomograms as optical ones, with the assumption inherently made in processing that the photons are reflected or scattered only once at the structure sensed. Thus, if a gradual decay of the signal is observed below the boundary of an opaque layer (see Figure 4a in Results section), it means that many multiscattering events occur in this layer and create a virtual downward elongation of the imaged stratum. In contrast, if the OCT signal decays rapidly, creating a narrow trail in a tomogram (see Figure 4b), it indicates that the layer absorbs light strongly. In neither of these cases, therefore, is it possible to determine the layer thickness.

Another consequence of the representation of distances as optical ones is that all of the internal structures of the object appear vertically stretched by a factor equal to the refractive index of the material. Consequently, as follows from eq 2, the axial resolution of the instrument is increased by the same factor. If the strata in the material examined are not perpendic-

ular to the beam direction, refraction of the incident and returning light also leads to some additional distortion of the image. It is possible to correct this effect numerically. However, in the cases of the tomograms presented in this Account, while exact image corrections were not performed, the vertical scale bar is adjusted to present what would, assuming a refractive index of 1.5 and no distortion by refraction, be real distances. In addition, the vertical scale of all tomograms presented is expanded with respect to the lateral scale, because this improves appreciation of the axial structure of the object.

Practical Examples

In this contribution, the results of OCT examinations made on two paintings on canvas of different style and time of origin are presented. The first depicts a Franciscan monk, Leonard of Porto Maurizio (1676–1751). In the lower right-hand corner, the painting bears an inscription (*St. Leonard*), and this is paired up with a date (1797) painted in the lower left-hand corner (Figure 2). It is known³⁶ that Leonard was beatified by Pope Pius VI in 1796, and proclaimed Saint by Pope Pius IX in 1867. This history has raised doubts about the origin of the inscriptions in the painting. If it had been executed in 1797, Leonard would not yet have been canonized. Thus it was reasonable to suspect that the inscription *St. Leonard* was added later.

An inspection of the picture in raking (obliquely incident) light revealed the existence of another inscription in the background, located above the date 1797 and hidden under a thick layer of varnishes and an overpainting. It was not possible to read particular letters with standard techniques; neither X-ray nor infrared examination had been helpful. Fortunately, the inscription was painted quite thickly, and the canvas and priming layers were thin enough to allow examination with white-light penetrating the picture from an intense source placed behind it (see Figure 6a in Results section). The two-line text could be deciphered as *B. Leonardus d.[a?] Maurizio*. However, it was not possible to determine the position of the inscription within the stratigraphy of the painting, which had been restored at least three times. It was therefore necessary more precisely to investigate the structure of the painting in order to verify the configuration of paint and varnish layers in the areas of all three inscriptions and thus provide unambiguous technical information with which to resolve its history.

The second painting examined dates from the late nineteenth century and depicts an unknown woman. It is skillfully painted and signed *GioRdi* (Figure 3). Routine inspection of UV-excited fluorescence of the painting proved the existence of two kinds of



FIGURE 2. *Saint Leonard of Porto Maurizio*, picture from the Franciscan Church of St. Bonaventure in Pakość, Poland, oil on canvas, $121 \times 84 \text{ cm}^2$, photography in front illumination, taken by Magdalena Iwanicka and used with permission. Circles mark the regions in which the tomograms shown in Figure 4 were taken. Rectangles mark the regions of the inscriptions investigated: tomograms shown in figures indicated.

varnish on its surface: primary, fluorescing yellow, and secondary, of slightly blue fluorescence. Although it is certain that such a difference in the color of fluorescence of two varnishes may be due only to their different composition, visual color impression alone (i.e., without precise spectroscopic analysis⁷) is not reliable for unambiguous identification of varnishes. However, some rough indication may be given by conservation practice: old oil-resin varnishes tend to fluoresce yellow-green, whereas modern synthetic varnishes develop rather blue fluorescence over time.

UV examination did not reveal any differences (which usually lead to the assumption of forgery) between the region of the signature and its surroundings. It can be seen in Figure 3 that the signature is placed within a strip-like area where the primary varnish had been removed before the whole painting (including the area of the signature) was covered with a different varnish, of rather blue UV-excited fluorescence. The aim of the OCT examination of the signature was to deter-

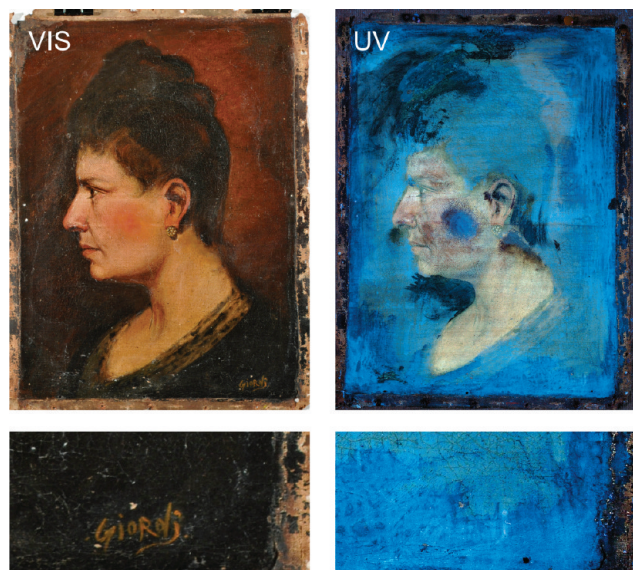


FIGURE 3. Upper panels, *Portrait of an unknown woman*, oil on canvas, $41.5 \times 30 \text{ cm}^2$, photography in front illumination (VIS) and of UV-excited fluorescence (UV); photo by W. Grzesik and used with permission. Lower panels: area of signature.

mine whether it lies on top of the remains of the original varnish (which had been removed), which would imply intentional forgery.

Results

a. Structural Imaging of Multilayer Paintings. The analysis of the painting *Saint Leonard of Porto Maurizio* by means of optical coherence tomography reveals quite a simple primary structure. In a sample tomogram (Figure 4a), no glaze layer is seen to be present, but up to four layers of varnish are revealed. They are distinguishable mostly due to particles of dirt originally present on the surface of the painting, which then became trapped under the next layer of varnish.³⁷ The signal from light scattered by these particles forms a line of dots in the tomogram, marking the location of the interface between the surface of the painting and the subsequent layers of varnish. Had the interface line in the tomogram been more continuous and better pronounced, reflection due to the difference in refractive indices would have been indicated.

The signal from scattering at the upper interface of the primary, most probably original, varnish layer (yellow arrows in the figure) is quite continuous, and the strongest of all those originating from interfaces between the varnish layers. This suggests that the painting was well dried, even weathered and not cleaned, before revarnishing. Such a structure is quite commonly present in OCT tomograms of varnish layers and may imply that such varnishes belong to different chronological phases.

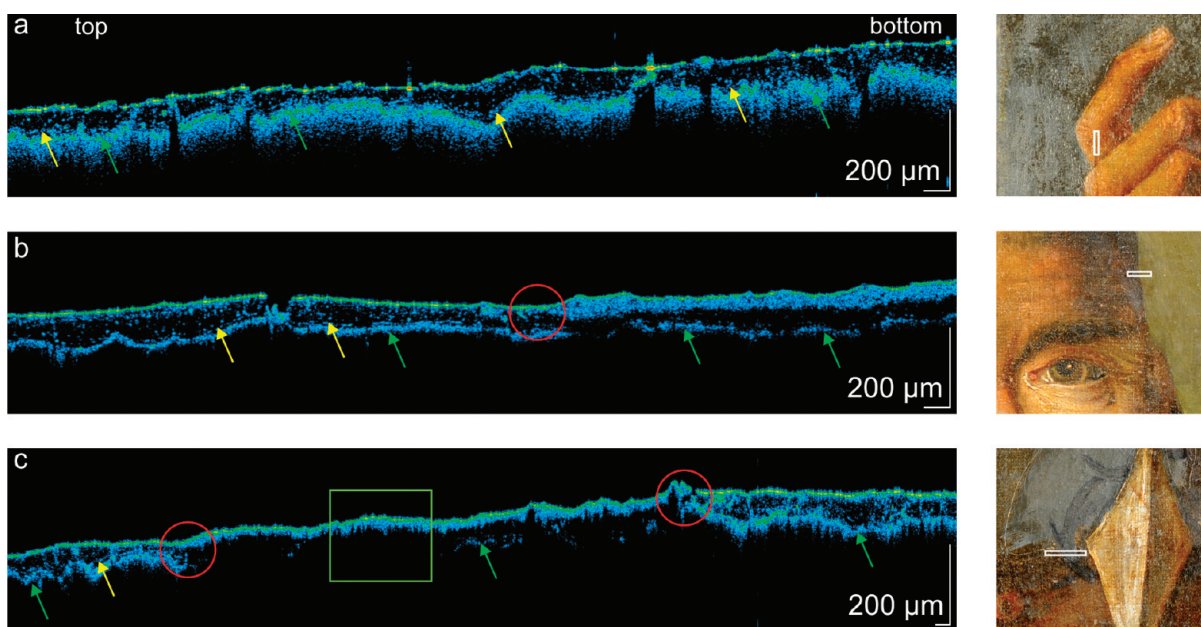


FIGURE 4. OCT tomograms from *Saint Leonard of Porto Maurizio*: (a) multilayer varnish (image width 7 mm); (b) semitransparent overpainting (image width 7 mm); (c) opaque overpainting (image width 12.3 mm). Yellow arrows indicate the surface of the primary varnish layer; green arrows indicate the primary opaque paint layer; circles show boundaries between original and overpainted areas; rectangle indicates a region in which the overpainting is completely opaque; see text for details. The bars indicate real distances in media of refractive index 1.5.

The opaque paint layer (green arrows) in the area of this tomogram absorbs the probing light moderately, and some residual multiscattering is present. In the next cross section (Figure 4b), the original paint layer (green arrows) is more absorbing, due to its different pigment composition, and thus visible as a narrow line. On the right-hand side, it is apparently covered by another layer of paint. It is clear that this paint layer, which is partially permeable to IR light, lies on at least three layers of varnish, and the original paint layer continues underneath. Such an OCT image is characteristic for

overpainting onto the surface of the picture. The practice of this kind of renovation was quite common in the past.

A similar situation is shown in Figure 4c, but the pigments in this overpainting absorb probing light strongly, and only traces of subsequent layers are visible. If only the part of this image marked with a green rectangle were analyzed separately, the image would suggest a nontransparent primary paint layer. However, detailed inspection in relation to the unaltered structures visible in Figure 4c outside the area of the overpainting, clearly indicates that, at the boundary between

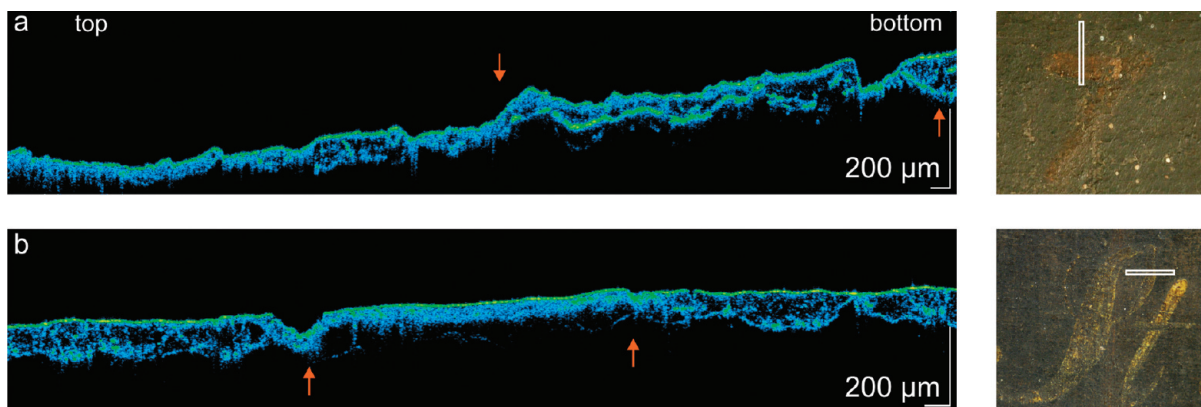


FIGURE 5. OCT examination of inscriptions from *Saint Leonard of Porto Maurizio*: (a) first digit 7 from date 1797 (image width 9.3 mm); (b) letter S from the text *St. Leonard*. (image width: 7 mm). Letters are located between arrows; see text for details. Bars indicate real distances in media of refractive index 1.5.

© Flow-through OCT movies of the first digit 7 from date 1797 and letter S from the text *St. Leonard* are available.

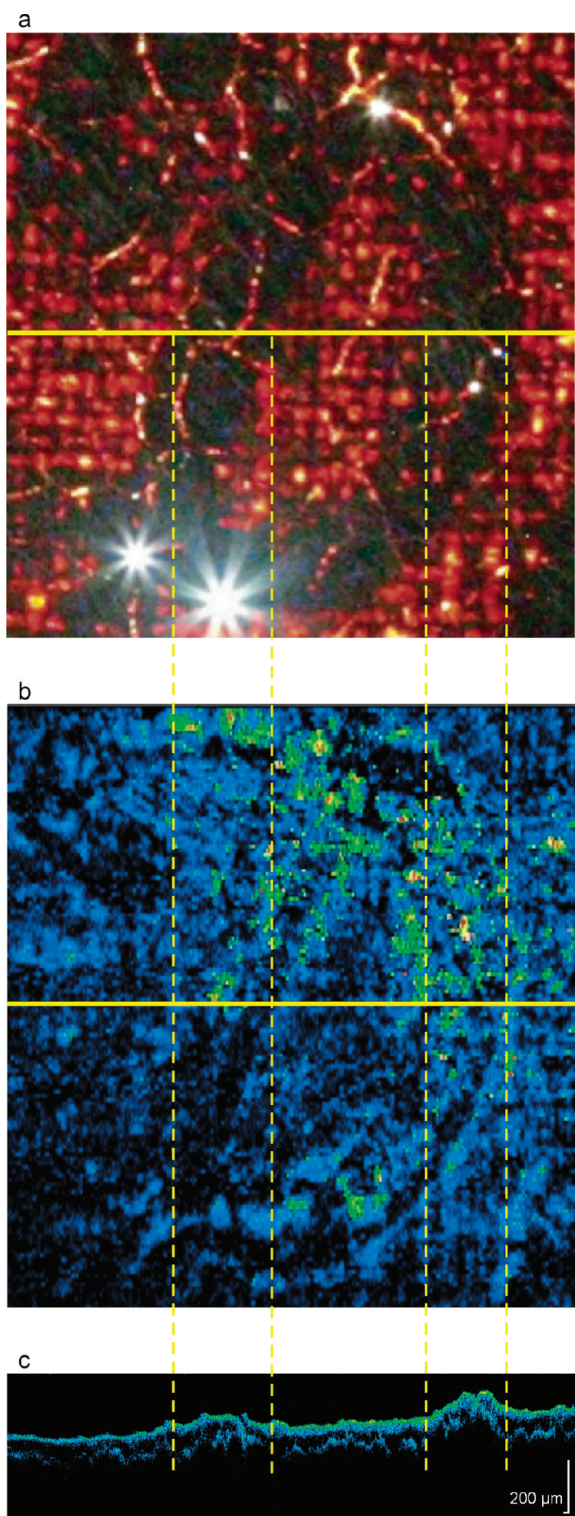


FIGURE 6. Analysis of the overpainted inscription *B Leonardus a Maurzio*: (a) letter *D* in intense penetrating light; (b) shape of the same letter reconstructed from the OCT data by extracting the signal from depths between 137 and 145 μm ; (c) the OCT scan in the same lateral scale. Yellow solid lines in panels a and b indicate the location of the scan.

the two areas (circles), the paint layers do not match and that the original layer (green arrows) extends underneath, similarly to that in Figure 4b.

Analyses of the kind described above may provide conservators with helpful information, which is especially important for the prospective removal of secondary layers to be carried out with the intention of preserving the original ones.

b. Analysis of Inscriptions and Artists' Signatures. A similar analysis applies to signatures and other inscriptions. The order of layers provides significant information on the painting's history and helps in understanding its origin. The painting *Saint Leonard of Porto Maurizio* is unsigned, as is often found in artworks commissioned by convents and painted by members of the community. As follows from the examination of the whole painting, sample results of which are shown in Figure 4, it was overpainted to a great extent at least twice and varnished at least three times. This condition must be taken into account when the properties of the inscriptions are examined.

In this picture, two texts are visible at present. One, 1797, refers to the possible year of its creation, the other, *St. Leonard.*, to the person depicted. Whereas the date is barely legible, and thus unfortunately not possible to reproduce here, the Saint's name is very clearly visible. Examination with the aid of OCT reveals a different localization of the two inscriptions within the stratigraphy of the painting. The date (Figure 5a, between arrows) is visible in the tomogram as a bright strip under the varnish and possibly under a semitransparent, thin overpainting covering all of the area under investigation. The exact position of the date within the structure is not entirely clear. It may be painted on top of the primary varnish (some traces of a transparent layer are visible underneath), but there is no doubt that the layer containing the date belongs to a deep stratum of the structure.

The second inscription (see letter *S* from *St. Leonard*, Figure 5b, between arrows) is painted on top of the thick coating of varnish covering the original black background which absorbs probing light strongly, so that only its upper interface is visible. The text *St. Leonard* must therefore be considered to have been added later, probably during the last renovation around the middle of the nineteenth century as an alteration commemorating Leonard's canonization.

The analysis of the third, overpainted, inscription proved much more difficult, since it is not legible directly, either by front illumination or in raking light, but photography with very strong back-lighting through the painting (Figure 6a) revealed shadows of the letters. Such imaging would not be possible, of course, in the case of a picture painted on a solid support, like a wooden panel. Because of the almost opaque overpainting layer covering the inscription, OCT examination of this area provided less than conclusive

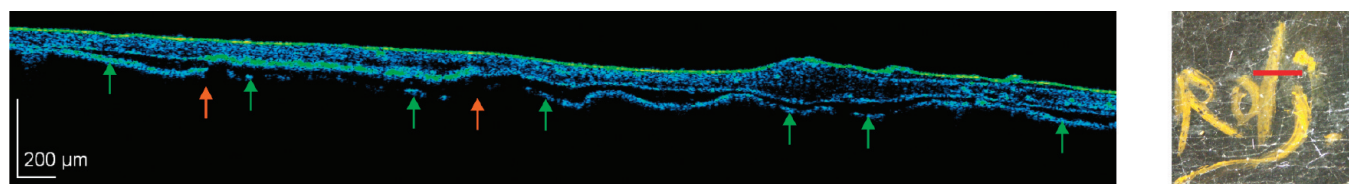


FIGURE 7. OCT tomogram from *Portrait of an unknown woman* taken over the letter *d* of the signature (located between red arrows). Green arrows indicate the primary, opaque paint layer. To the right, three layers of varnish are visible over an opaque paint layer. Bars indicate real distances in media of refractive index 1.5.

direct results. The deciphering of the letters from 3-D OCT was, nevertheless, possible (Figure 6b) by adding together signals from defined depths beneath the surface and presenting them in a false-color scale, a procedure that had previously been tested and proved²⁷ on model paintings. In the present case, the greatest legibility was obtained by visualization of shadows of the thick letters, that is, by collecting signal from underneath the paint layer (137–145 μm). It should be emphasized that, since this technique utilizes scattered light, it is not limited to paintings on transparent supports. Moreover, careful inspection of this OCT tomogram (Figure 6c) leads to the conclusion that the whole area of investigation is, as expected, covered by the overpainting, with a continuous layer of varnishes underneath. It is important to note that, in the tomogram, the layer of varnishes in areas that correspond to cross sections of the letter *D* is visually similar to that in the surrounding background; no shadows cast by the opaque paint of the inscription are present. Thus, the different transparency of the structure, which made it possible to obtain an image from Figure 6a, is not induced by the top layers of the painting. This means that the inscription must be located underneath the subsequent layer of varnish. However, it is not visible as a separate stratum. This effect may be explained by the strong absorption of light in the thick body of this paint (confirmed by inspection of the image in Figure 6a), which, together with signal loss in the overpainting located on the painting surface, renders it impossible to see much of anything below the varnish layer.

Taken together, the detailed conclusions concerning the inscriptions in this picture lead to the supposition that the work may have been painted at some time in the year after Leonard's beatification in 1796. At that time, the picture carried the inscription *B. Leonardus d.[a?] Maurzio*, with both the date and the caption covered by a thick multiple layer of varnishing. Subsequently, after canonization, the original inscription was painted over and a new, updated, one added. The date was left visible, possibly even emphasized by overpainting it.

In the second case study, *Portrait of an unknown woman*, the OCT examination shows two layers of varnish (Figure 7): a clear lower layer and a more scattering upper one. This confirms the results of the inspection of the painting's surface by UV-excited fluorescence (Figure 3), which had revealed the existence of two different kinds of varnish. The primary, probably original, varnish had been partially removed, but its residue is clearly seen in Figure 7. There is no doubt that the signature lies on top of the primary layer of varnish, because the thin opaque paint layer of the signature (between arrows in Figure 7) is located at precisely the same level as the interface between the two varnishes. Moreover, although the paint layer of the signature obstructs deeper penetration of the beam, some traces of the original paint layer (marked with green arrows in Figure 7) are visible underneath at a distance corresponding to the thickness of the primary varnish in the proximity. This analysis suggests that the signature is a forgery: it leads to the strong suspicion that removal of the original varnish, of yellow UV-excited fluorescence, was intentional, and carried out in order to create the impression that the forged signature was a genuine original one placed directly on the paint layer before any varnishing.

Summary

The aim of this Account has been to show, using examples of studies of original paintings, the potential of optical coherence tomography for solving real problems arising in art conservation studios. The investigation of inscriptions on oil paintings was specifically discussed. For two examples of such paintings, it has been demonstrated that examination by OCT permits the localization of particular paint layers within the stratigraphy of the thin structure of the paintings. If this structure is transparent enough to the infrared light used for the examination, OCT may constitute the optimal method of choice for cross-sectional examination because of its noninvasiveness, which allows its unrestricted use even in such sensitive areas as those of the artist's signature. Despite the very specific subject of the studies reported here, it is evident that

the kind of approach described in this Account may easily be adaptable to other appropriately similar tasks in forensic or materials science.

In the authors' opinion, the most promising approach is a synergistic one in which the information gained by means of various different noninvasive methods is combined. Among these methods, OCT shows great potential for further application and development.

The authors are grateful to Dr. Robert Dale for critical reading of the manuscript and a number of useful comments. This work was supported by Polish Government Research Grants through the years 2008–2011. M.I., E.A.K., and M.S. gratefully acknowledge additional support from the European Social Fund and the Polish Government within their Integrated Regional Development Operational Program, Action 2.6, under the project "Stypendia dla doktorantów 2008/2009 - ZPORR" of the Kuyavian-Pomeranian Voivodship. M.I. additionally acknowledges support from the Foundation for Polish Science within the Ventures Program cofinanced by Operational Programme Innovative Economy within the European Regional Development Fund.

BIOGRAPHICAL INFORMATION

Piotr Targowski is a Professor of Optics and Informatics in the Institute of Physics of the Nicolaus Copernicus University.

Magdalena Iwanicka is a Ph.D. student in the Institute for the Study, Restoration and Conservation of Cultural Heritage of the Nicolaus Copernicus University and a Foundation of Polish Science scholar.

Ludmiła Tymińska-Widmer is an assistant lecturer at the Institute for the Study, Restoration and Conservation of Cultural Heritage of the Nicolaus Copernicus University.

Marcin Sylwestrzak is a Ph.D. student in the Institute of Physics of the Nicolaus Copernicus University.

Ewa A. Kwiatkowska is a Ph.D. student in the Institute of Physics of the Nicolaus Copernicus University.

REFERENCES

- 1 de la Rie, E. R. The influence of varnishes on the appearance of paintings. *Stud. Conserv.* **1987**, *32*, 1–13.
- 2 Berns, R. S.; de la Rie, E. R. Exploring the optical properties of picture varnishes using imaging techniques. *Stud. Conserv.* **2003**, *48*, 73–82.
- 3 Plesters, J. Cross-sections and chemical analysis of paint samples. *Stud. Conserv.* **1956**, *2*, 110–157.
- 4 van der Weerd, J. Microspectroscopic analysis of traditional oil paint, Ph.D. Thesis, FOM Institute for Atomic and Molecular Physics, Amsterdam, 2002 <http://www.amolf.nl/publications/theses/after-2000/> (accessed 07/03/2009).
- 5 Rouba, B.; Karaszkiewicz, P.; Tymińska-Widmer, L.; Iwanicka, M.; Góra, M.; Kwiatkowska, E.; Targowski, P. Optical coherence tomography for non-destructive investigations of structure of objects of art. Presented at the 9th International Conference on Non Destructive Testing of Art, Jerusalem, Israel, May 25–30, 2008, <http://www.ndt.net/article/art2008/papers/143Targowski.pdf> (accessed 07/03/2009).
- 6 de la Rie, E. R. Fluorescence of paint and varnish layers, Part I, II, III. *Stud. Conserv.* **1982**, *17*, 1–7; 65–69; 102–108.
- 7 Thoury, M.; Elias, M.; Frigerio, J. M.; Barthou, C. Nondestructive varnish identification by ultraviolet fluorescence spectroscopy. *Appl. Spectrosc.* **2007**, *61*, 1275–1282, 10.1366/000370207783292064.
- 8 Dupuis, G.; Elias, M.; Simonot, L. Pigment identification by fiber-optics diffuse reflectance spectroscopy. *Appl. Spectrosc.* **2002**, *56*, 1329–1336, 10.1366/00037020760354803.
- 9 Van Asperen de Boer, J. Infrared reflectography: A method for the examination of paintings. *Appl. Opt.* **1968**, *7*, 1711–1714.
- 10 Gavrilov, D.; Ibarra-Castanedo, C.; Maeva, E.; Grube, O.; Maldague, X.; Maev, R. G. Infrared methods in noninvasive inspection of artwork. Presented at 9th International Conference on NDT of Art, Jerusalem, Israel, May 25–30, 2008, <http://www.ndt.net/article/art2008/papers/040Gavrilov.pdf> (accessed 07/03/2009).
- 11 Maev, R. G.; Gavrilov, D.; Maeva, A.; Vodyanoy, I. Modern non-destructive physical methods for paintings testing and evaluation. Presented at 9th International Conference on Non Destructive Testing of Art, Jerusalem, Israel, May 25–30, 2008, <http://www.ndt.net/article/art2008/papers/042Maev.pdf> (accessed 07/03/2009).
- 12 Tornari, V. Optical and digital holographic interferometry applied in art conservation structural diagnosis. *e-Preserv. Sci.* **2006**, *3*, 51–57.
- 13 Complete list of papers on application of OCT to examination of artwork may be found at <http://www.oct4art.eu> (accessed 07/03/2009).
- 14 Targowski, P.; Rouba, B.; Wojtkowski, M.; Kowalczyk, A. The application of optical coherence tomography to non-destructive examination of museum objects. *Stud. Conserv.* **2004**, *49*, 107–114.
- 15 Liang, H.; Cid, M.; Cucu, R.; Dobre, G.; Podoleanu, A.; Pedro, J.; Saunders, D. En-face optical coherence tomography—a novel application of non-invasive imaging to art conservation. *Opt. Express* **2005**, *13*, 6133–6144, 10.1364/OPEX.13.006133.
- 16 Arechchi, T.; Bellini, M.; Corsi, C.; Fontana, R.; Materazzi, M.; Pezzati, L.; Tortora, A. A new tool for painting diagnostics: Optical coherence tomography. *Opt. Spectrosc.* **2006**, *101*, 23–26, 10.1134/S0030400X06070058.
- 17 Latour, G.; Georges, G.; Siozade, L.; Deumie, C.; Echard, J. P. Study of varnish layers with optical coherence tomography in both visible and infrared domains. *Proc. SPIE* **2009**, *7391*, 73910J, 10.1117/12.827856.
- 18 Latour, G.; Moreau, J.; Elias, M.; Frigerio, J.-M. Optical Coherence Tomography: non-destructive imaging and spectral information of pigments. *Proc. SPIE* **2007**, *6618*, 661806, 10.1117/12.726084.
- 19 Yang, M. L.; Lu, C. W.; Hsu, I. J.; Yang, C. C. The use of optical coherence tomography for monitoring the subsurface morphologies of archaic jades. *Archaeometry* **2004**, *46*, 171–182, 10.1111/j.1475-4754.2004.00151.x.
- 20 Yang, M.-L.; Winkler, A. M.; Barton, J. K.; B., V. P. Using optical coherence tomography to examine the subsurface morphology of Chinese glazes. *Archaeometry* **2008**, *51*, 808–821.
- 21 Liang, H.; Peric, B.; Hughes, M.; Podoleanu, A. G.; Spring, M.; Roehrs, S. Optical coherence tomography in archaeological and conservation science - a new emerging field. *Proc. SPIE* **2008**, *7139*, 713915, 10.1117/12.819499.
- 22 Kunicki-Goldfinger, J.; Targowski, P.; Góra, M.; Karaszkiewicz, P.; Dzierzanowski, P. Characterization of glass surface morphology by optical coherence tomography. *Stud. Conserv.* **2009**, *54*, 117–128.
- 23 Adler, D. C.; Stenger, J.; Gorczynska, I.; Lie, H.; Hensick, T.; Spronk, R.; Wolohojian, S.; Khandekar, N.; Jiang, J. Y.; Barry, S. Comparison of three-dimensional optical coherence tomography and high resolution photography for art conservation studies. *Opt. Express* **2007**, *15*, 15972–15986, 10.1364/OE.15.015972.
- 24 Liang, H.; Cid, M.; Cucu, R.; Dobre, G.; Kudimov, B.; Pedro, J.; Saunders, D.; Cupitt, J.; Podoleanu, A. Optical coherence tomography: A non-invasive technique applied to painting conservation of paintings. *Proc. SPIE* **2005**, *5857*, 261–269.
- 25 Targowski, P.; Góra, M.; Wojtkowski, M. Optical coherence tomography for artwork diagnostics. *Laser Chem.* **2006**, *2006*, 1–11, 10.1155/2006/35373. <http://www.hindawi.com/journals/lc/2006/035373.abs.html>, (accessed 07/03/2009).
- 26 Góra, M.; Targowski, P.; Rycyk, A.; Marczał, J. Varnish ablation control by optical coherence tomography. *Laser Chem.* **2006**, *2006*, 1–7, 10.1155/2006/10647. <http://www.hindawi.com/journals/lc/2006/010647.abs.html>, (accessed 07/03/2009).
- 27 Targowski, P.; Rouba, B.; Góra, M.; Tymińska-Widmer, L.; Marczał, J.; Kowalczyk, A. Optical coherence tomography in art diagnostic and restoration. *Appl. Phys. A: Mater. Sci. Process.* **2008**, *92*, 1–9, 10.1007/s00339-008-4446-x.
- 28 Góra, M.; Targowski, P.; Kowalczyk, A.; Marczał, J.; Rycyk, A. Fast spectral optical coherence tomography for monitoring of varnish ablation process. In *Lasers in the Conservation of Artworks*, LACONA VII Proceedings, Madrid, Spain, Sept. 17–21, 2007; Castillejo, M., Ed.; Taylor & Francis Group: London, 2008; pp 23–26.
- 29 Targowski, P.; Góra, M.; Bajraszewski, T.; Szkulmowski, M.; Rouba, B.; Łekawa-Wysłouch, T.; Tymińska, L. Optical coherence tomography for tracking canvas

- deformation. *Laser Chem.* 2006, **2006**, DOI: 10.1155/2006/93658, <http://www.hindawi.com/journals/lc/2006/093658.abs.html> (accessed 07/03/2009).
- 30 *Optical Coherence Tomography: Technology and Applications*; Drexler, W., Fujimoto, J. G., Eds.; Springer-Verlag: Berlin, Heidelberg, New York, 2008.
- 31 Dubois, A.; Grieve, K.; Moneron, G.; Lecaque, R.; Vabre, L.; Boccara, C. Ultrahigh-resolution full-field optical coherence tomography. *Appl. Opt.* **2004**, *43*, 2874–2883.
- 32 Dubois, A.; Moreau, J.; Boccara, C. Spectroscopic ultrahigh-resolution full-field optical coherence microscopy. *Opt. Express* **2008**, *16*, 17082–17091, 10.1364/OE.16.017082.
- 33 Fercher, A. F. Optical coherence tomography. *J. Biomed. Opt.* **1996**, *1*, 157–173, 10.1117/12.231361.
- 34 Leitgeb, R.; Hitzenberger, C. K.; Fercher, A. F. Performance of Fourier domain vs. time domain optical coherence tomography. *Opt. Express* **2003**, *11*, 889–894.
- 35 Sylwestrzak, M.; Kwiatkowska, E. A.; Karaszkiewicz, P.; Iwanicka, M.; Targowski, P. Application of graphically oriented programming to imaging of structure deterioration of historic glass by optical coherence tomography. *Proc. SPIE* **2009**, *7391*, 739109, 10.1117/12.827520.
- 36 Bihl, M. St Leonard of Port Maurice. The Catholic Encyclopedia 1910, Vol. 9, <http://www.newadvent.org/cathen/09178c.htm> (accessed 07/03/2009).
- 37 Stifter, D.; Sanchis Dufau, A. D.; Breuer, E.; Wiesauer, K.; Burgholzer, P.; Höglinger, O.; Götzinger, E.; Pircher, M.; Hitzenberger, C. K. Polarisation-sensitive optical coherence tomography for material characterisation and testing. *Insight - Non-Destruct. Test. Cond. Monit* **2005**, *47*, 209–212, 10.1784/insi.47.4.209.63154.